

# Probing Relativistic Spin Effects in the Nucleon by Means of Drell-Yan Processes

F. Cano<sup>1</sup>, P. Faccioli<sup>2</sup> and M. Traini<sup>1,3</sup>

<sup>1</sup>Dipartimento di Fisica  
Università degli Studi di Trento  
I-38050 Povo, Italy

<sup>2</sup>ECT\*,  
(European Centre for Theoretical Nuclear Physics and Related Areas),  
Villa Tambosi, I-38050 Villazano (Trento), Italy

<sup>3</sup>Istituto Nazionale di Fisica Nucleare, G.C. Trento.

## Abstract

Significant differences between transverse and longitudinal polarized parton distributions are found at low energies within a light-front covariant quark model of the nucleon. These differences are due to relativistic spin effects introduced by the Melosh rotations and survive evolution to higher  $Q^2$  scales. We show that the importance of these relativistic effects can be assessed by measuring double-spin asymmetries in lepton pair production in polarized hadron-hadron collisions.

PACS: 12.39.-x, 12.39.Ki, 13.88.+e

Keywords: Drell-Yan Processes, light-front models, transversity.

cano@science.unitn.it  
traini@science.unitn.it  
faccioli@ect.unitn.it

Preprint U T F / 99-430, E C T \* / 01-99

# 1 Introduction

A complete description of the momentum and spin degrees of freedom of quarks and antiquarks in the nucleon requires, at leading twist, the definition of three sets of parton distributions. Two of them, the momentum distribution  $f(x; Q^2)$  and the helicity distribution  $g_1(x; Q^2)$  have been widely studied and measured [1, 2]. The third one, the so called transversity distribution  $h_1(x; Q^2)$ , has come to the attention of theorists and experimentalists quite recently in the analysis of Drell-Yan spin asymmetries in 1979 [3]. The main reason why it has passed unnoticed for such a long time is its chiral-odd character. If quark mass terms in the QCD Lagrangian are neglected, there is no interaction at lowest order of perturbation theory that can flip chirality. As a consequence, transversity is strongly suppressed (by powers of  $m_q/Q$ ) in deep inelastic lepton-nucleon scattering (DIS) and in general in any hard process that involves only one parton distribution. In Drell-Yan processes the chirality of the partons that annihilate is uncorrelated and the restrictions mentioned above do not apply.

Recently there has been a few proposals to measure the transversity parton distributions (see [4] for a review). Hadron-hadron doubly polarized collisions are among the most promising reactions to extract information about transversity and such experiments are already included in the research program at RHIC and HERA [5]. From the cross section of D-Y processes it is possible to build an observable, the double transverse asymmetry, proportional to the transversity parton distribution  $h_1$

$$A_{TT} = \frac{d(\uparrow\uparrow) - d(\uparrow\downarrow)}{d(\uparrow\uparrow) + d(\uparrow\downarrow)} = \frac{\sin^2 \theta \cos 2\phi}{1 + \cos^2 \theta} \frac{\sum_a e_a^2 h_1^a(x_1; Q^2) h_1^a(x_2; Q^2)}{\sum_a e_a^2 f_1^a(x_1; Q^2) f_1^a(x_2; Q^2)} + (x_1 \leftrightarrow x_2) \quad (1)$$

where the arrows denote the transverse polarization of the beam and target,  $\theta$  is the polar (azimuthal) angle of the detected lepton,  $e_a$  is the charge of a quark with flavor  $a$  and  $Q^2$  is the invariant mass of the produced lepton pair. With respect to the argument of the distribution functions in (1),  $x_1$  and  $x_2$  are related to the kinematic variables:

$$x_1 = \frac{r}{s} \frac{Q^2}{e^y}; \quad x_2 = \frac{r}{s} \frac{Q^2}{e^{-y}} \quad (2)$$

where  $\frac{r}{s}$  is the center of mass energy and  $y$  is defined in terms of the components of the four-momentum of the pair:  $y = \text{arctanh}(Q^3/Q^0)$ .

Additionally, it is useful to define another asymmetry that can be measured with longitudinally polarized hadrons and is proportional to the helicity distribution  $g_1$ :

$$A_{LL} \frac{d(\sigma_{\parallel})}{d(\sigma_{\parallel}) + d(\sigma_{\#})} = \frac{\sum_a e_a^2 g_1^a(x_1; Q^2) g_1^a(x_2; Q^2)}{\sum_a e_a^2 f_1^a(x_1; Q^2) f_1^a(x_2; Q^2)} + (x_1 \otimes x_2) \quad (3)$$

The arrows in (3) indicate longitudinal polarization of the beam and the target.

Along with the encouraging experimental prospects, many efforts have also been made on the theoretical side [6, 7, 8, 9, 10, 11]. Jaffe and Ji have given predictions for  $h_1$  in the bag model [6], pointing out the relativistic character of the differences between transverse and longitudinal polarization properties. Other relativistic effects (due to Melosh rotations) have also been investigated for the transversity [7] and for the tensor charge (analogous to the axial charge in longitudinal polarization) [8].

The calculation of the anomalous dimensions at leading order (LO) [12] and next-to-leading order (NLO) [13] allowed to address quantitatively the differences between  $g_1$  and  $h_1$  due to perturbative QCD (pQCD) evolution in different models [9, 10]. In particular, it has been shown [9, 10] that these differences are sizeable only in the small  $x$  region ( $x \lesssim 0.1$ ).

On the other hand the boundary conditions of the evolution equations, that are provided by the low energy input at the hadronic scale  $Q_0^2$  ( $\sim 1 \text{ GeV}^2$ ), can yield to an additional, non-perturbative, difference. As it was stressed by Jaffe [6], at this scale the equality  $h_1(x; Q_0^2) = g_1(x; Q_0^2)$  is a typical outcome of non-relativistic models of the nucleon, in which motion and spin observables are uncorrelated. In other words, any departure from the previous identity is a signature of relativity in the employed hadronic model.

Our goal is a quantitative study of the relativistic effects due to the correlations between spin and motion in hadronic systems. For this purpose, we have used light-front dynamics formalism, in which the interplay between motion and spin is made explicit through the Melosh rotations. In particular, we have used the light-front covariant (LFC) quark model of ref. [14] to compute the leading twist contribution to the hadronic matrix elements at the scale  $Q_0^2$ . This non-perturbative input has been then evolved at NLO up to a higher  $Q^2$  scale. We shall show that these relativistic corrections at  $Q_0^2$  clearly survive evolution. Measurements of the asymmetries (1), (3) in a feasible kinematic regime may decide on the relevance of these corrections to the naive non-relativistic spin picture adopted in low-energy models of the nucleon.

## 2 Polarized parton distributions in a LFC quark model

The helicity distribution  $g_1^a(x; Q^2)$  of a parton with flavour  $a$  is defined as the probability of having a (longitudinally) polarized parton  $a$  with spin parallel

to the longitudinal polarization of the parent nucleon minus the probability of finding the parton polarized in the opposite direction. A similar definition applies to  $h_1(x; Q_0^2)$  with transverse polarizations instead of longitudinal ones [2].

One central assumption in the approach developed in [14, 15] is that the hadronic scale  $Q_0^2$  can be chosen in such a way that only valence degrees of freedom affect the calculation of the hadron matrix elements at leading twist. Therefore, according to the previous definitions we can write:

$$xg_1^a(x; Q_0^2) = \frac{x}{(1-x)^2} \int_{-Z}^Z d^3k (n_a''(\vec{k}) - n_a^\#(\vec{k})) \frac{x}{1-x} \frac{k^+}{M = \frac{P^-}{2}} \quad (4)$$

$$xh_1^a(x; Q_0^2) = \frac{x}{(1-x)^2} \int_{-Z}^Z d^3k (n_a'(\vec{k}) - n_a(\vec{k})) \frac{x}{1-x} \frac{k^+}{M = \frac{P^-}{2}} \quad (5)$$

where  $\vec{k}_q$  is the three-momentum of the struck quark,  $M$  is the nucleon mass,  $k^+ = (\vec{k}^2 + m_q^2 + k_z) = \frac{P^-}{2}$  and  $n_a^{\#(\prime)}(\vec{k})$  is the density of (valence) quarks with momentum  $\vec{k}$  and longitudinal polarization aligned (antialigned) with the longitudinal polarization of the parent nucleon. A similar notation ( $n_a'(\vec{k})$ ) is used for transverse polarization. The explicit expressions for the densities are:

$$n_a^{\#}(\vec{k}) = \int_{i=1}^X hP; S_z = +1=2j \ P_i^a \frac{1}{2} \frac{z^{(i)}}{2} \ \vec{k} \ \vec{k}_i) \mathcal{P}; S_z = +1=2i \quad (6)$$

$$n_a'(\vec{k}) = \int_{i=1}^X hP; S_x = +1=2j \ P_i^a \frac{1}{2} \frac{x^{(i)}}{2} \ \vec{k} \ \vec{k}_i) \mathcal{P}; S_x = +1=2i \quad (7)$$

where  $P_i^a$  is the flavour projector.

It is clear that in any non-relativistic description of the wave function the densities (6) and (7) are equal and hence  $h_1(x; Q_0^2) = g_1(x; Q_0^2)$ . In the covariant quark models based on light-front dynamics this is not necessarily the case, and departures from this equality are expected.

Light-front dynamics treatment of systems with a fixed number of particles has been widely discussed in the literature (see [16] for a review), so that it is enough to highlight briefly the main features of the angular momentum in this formalism. In the light-front form of the dynamics, the angular momentum operator for a single free particle is obtained by a combination of generators of Poincare group satisfying ordinary SU(2) algebra. However, when considering systems with more than one particle, usual composition rules for the individual angular momenta are not satisfied. Nevertheless, it is possible to restore

them by means of a unitary transformation: the (generalized) Melosh rotation [17]. From the physical viewpoint these transformations relate the angular momentum eigenstates in a subsystem rest frame (a quark, for example) to the centre of mass frame. For spin 1/2 particles the Melosh rotation (MR) that links light-front to canonical spin states is represented by:

$$D^{1=2} [R_M(\vec{k})] = \frac{(m + \not{k}_z) \not{\epsilon} (\not{1} - \not{k}_z)}{((m + \not{k}_z)^2 + \vec{k}_\perp^2)^{1=2}} \quad (8)$$

where  $\vec{k}$  is the three momentum of the particle and  $\not{k} = \gamma^\mu k_\mu$  its relativistic energy. The fact that  $D^{1=2} [R_M(\vec{k})] \rightarrow 1$  in the limit  $\vec{k}_\perp \rightarrow 0$  reveals the relativistic origin of the Melosh rotation.

In our calculation we shall refer to the wave function obtained in [14], adding to the free relativistic mass operator  $M_0 = \sum_{i=1}^3 \not{\epsilon}_i$  an hypercentral phenomenological interaction:

$$V = -\frac{1}{\Lambda} + \frac{1}{\Lambda} \quad (9)$$

where the hyper-radius  $r^2 = \sum_{i=1}^3 (\vec{r}_i - \vec{R})^2$  is a function of what, in a non relativistic treatment, is the vector position of the particles  $\vec{r}_i$  and the center of mass position  $\vec{R}$ .  $\Lambda$ ,  $\alpha$  and  $\beta$  are constants fixed to reproduce the basic features of the low-energy baryonic spectrum pattern in the  $J^P = 1=2$  channels. The outstanding advantage of the hypercentral interaction [18] is that they allow a straightforward solution of the mass equation. The resulting spin-isospin wave function is SU(6) symmetric. Notice that, since this interaction is invariant under rotations and does not depend on the total light-front momentum, all the commutation relations that guarantee the covariance requirement (see [16]) are correctly satisfied.

As a consequence of the presence of Melosh rotations in the spin sector, a relativistic factor appears and the densities (6) and (7) are no longer equal. Differences between  $h_1(x; Q_0^2)$  and  $g_1(x; Q_0^2)$  are now proportional to  $\vec{k}_\perp$ , as expected:

$$\begin{aligned} x h_1^u(x; Q_0^2) - x g_1^u(x; Q_0^2) &= \frac{4}{Z} (x h_1^d(x; Q_0^2) - x g_1^d(x; Q_0^2)) \quad \# \\ &= \frac{x}{(1-x)^2} \int d^3k \frac{4 \vec{k}_\perp^2}{9 ((m + \not{k}_z)^2 + \vec{k}_\perp^2)} \\ n(\vec{k}) &= \frac{x}{1-x} \frac{k^+}{M = \frac{P}{2}} \quad (10) \end{aligned}$$

where  $n(\vec{k})$  is the unpolarized flavorless quark momentum density normalized to the number of particles. A relationship similar to (10) was found by M a

et al. [7] in the Light-Cone SU(6) spectator model. One should keep in mind however that the MR is not the unique source of differences between  $h_1$  and  $g_1$  since they also differ in the anomalous dimensions used in evolution.

### 3 Results and discussion

To reach the experimental regime we have evolved the calculated parton distributions from the hadronic scale up to a scale  $Q^2 > Q_0^2$  by using pQCD at NLO, in the  $\overline{MS}$  scheme. The sensitivity to the factorization scheme in this approach has been tested in previous calculations [14] and found to be small.

The value of  $Q_0^2$  at the hadronic scale is fixed by evolving backwards the parametrized experimental fits for unpolarized parton distributions [19], to the scale where the valence quarks carry all the momentum of the nucleon. We found  $Q_0^2 = 0.094 \text{ GeV}^2$ . The reliability of the pQCD evolution procedure at such low scale was studied in detail in [9, 14, 15]. A few comments are in order: i) First, the running coupling constant at NLO must be obtained by solving the complete transcendental equation derived from RGE [20] and not from approximate high- $Q^2$  expressions [21]; ii) On the other hand, the evolution equations must have complete symmetry between  $Q^2$  and  $Q_0^2$  so that approximations due to Taylor expansions of the genuine pQCD series must be avoided.

In fig. 1 we show the curves for  $h_1^u$  and  $g_1^u$  at the hadronic scale  $Q_0^2$  (fig. 1a) and at the partonic scale  $Q^2 = 100 \text{ GeV}^2$  (fig. 1b). A remarkable difference between  $h_1(x; Q_0^2)$  and  $g_1(x; Q_0^2)$  appears now at large  $x$ , reaching its peak at  $x \approx 0.5$ . Quantitatively they are bigger than those obtained with the bag model [6, 9]. In any case, it is clear that the probability of transverse polarization is larger than the longitudinal one when relativistic effects are considered. It is possible to appreciate better the MR effects by simply setting  $D^{1=2} [R_M(k)] \equiv 1$ . The obtained results are also shown in fig. 1a. At the hadronic scale then we get  $h_1(x; Q_0^2) = g_1(x; Q_0^2)$  as expected. After evolution, in fig. 1b, we see that when the MR is not present, differences between  $h_1$  and  $g_1$  are mainly concentrated at low  $x$  ( $x < 0.1$ ). With the MR these differences, aside from its quantitative value at low  $x$ , also appear in the medium and large  $x$  region.

In Deeply Inelastic lepton pair production the observables that can be measured are the asymmetries (1), (3). The ratio between them does not depend on the unpolarized parton distribution and to this respect is less model dependent and more transparent to MR effects. In fig. 2 the ratio,

$$R_A(x_1; x_2; Q^2) = \frac{A_{TT}}{A_{LL}} \frac{1}{f(x; y)} = \frac{P}{P_a} \frac{e_a^2 h_1^a(x_1; Q^2) h_1^a(x_2; Q^2)}{e_a^2 g_1^a(x_1; Q^2) g_1^a(x_2; Q^2)} + (x_1 \neq x_2); \quad (11)$$

is plotted as a function of the center of mass rapidity  $y$  in a kinematic region ( $\sqrt{s} = 100 \text{ GeV}$ ,  $Q^2 = 100 \text{ GeV}^2$ ) which will be accessible by RHIC experiments. Again it is possible to single out the modifications due to MR by switching it off.

Figure 2 represents our main result: relativistic spin effects produce an enhancement of the transverse asymmetry against the longitudinal one. Namely, if MR are taken into account, we have that, in the considered kinematic region,  $(A_{TT} = f(x; y))' > A_{LL}$ . On the other hand, if the spin wave function undergoes no MR (i.e. in its non-relativistic limit), then in the same region we have  $(A_{TT} = f(x; y))' < \frac{1}{2} A_{LL}$ . Experiments may decide between these two alternatives, therefore probing the relevance of covariance effects in the dynamical description of the nucleon spin.

At this point one can argue that these results could be strongly influenced by the presence of high momentum components in the spatial part of the wave function, carried over by the presence of a relativistic kinetic energy in the mass operator. These components have been proved to be essential to describe electromagnetic transitions and elastic form factors [23] and also the high  $x$  region in DIS [14, 15]. We have therefore repeated the calculation of the ratio  $R_A(x_1; x_2; Q^2)$  starting from a nucleon wave function obtained with a non-relativistic kinetic energy in the mass operator. The interaction has been kept of the same form (9), while the values of the parameters ( $\alpha, \beta, \gamma$ ) have been reset according to ref [14].

The corresponding result for  $R_A(x_1; x_2; Q^2)$  is displayed in Fig. 2. We can see that the ratio obtained from a fully non-relativistic model, lies reasonably close to the curve obtained employing a relativistic kinetic energy but no MR. Hence, we can safely conclude that  $R_A(x_1; x_2; Q^2)$  is rather insensitive to the details of the mass operator, but very sensitive to the relativistic spin corrections derived from a light-front dynamics. This is not so evident for the values of  $A_{TT}$  and  $A_{LL}$  separately, supporting the suitability of the chosen observable. Moreover, due to this insensitivity to the details of the spatial wave function, we do not expect a dramatic change of our conclusions for other more sophisticated potential models in the market [22].

The range of  $x$  values covered in Fig. 2,  $0.03 < x < 0.27$ , is a relatively safe region for the numerical calculations (Mellin inversion) in the evolution procedure. But experimental data are not taken at a fixed  $Q^2$  as shown in Fig. 2. In Figure 3 we show the ratio  $R_A(x_1; x_2; Q^2)$  as a function of the invariant mass of the lepton pair  $Q^2$  at a fixed rapidity  $y = 0$  (i.e.  $x_1 = x_2$ ). The effect of the Melosh rotation and the relative insensitivity to the details of the chosen

potential are evident also in this representation.

Summarizing, we have shown that, by means of Drell-Yan processes, it is possible to probe the light-front dynamical description of the low energy spin structure of the nucleon. For this purpose, the ratio  $A_{TT}=A_{LL}$  turns out to be particularly suitable since it is not essentially affected by the structure of the mass operator and, therefore, by the choice of the phenomenological interaction. We have presented the predictions for this observable in a feasible kinematic regime. If Melosh rotations are considered this ratio is approximately 1, while if they are neglected (as in the non relativistic description) the same ratio is around 0.5.

We are grateful to S. Scopetta for useful suggestions and for providing us with an updated version of the pQCD evolution code. We thank V. Vento for his encouragement and help during the present study and for a critical reading of the manuscript. We also thank M. Miyama for sending us his evolution code for  $h_1$  of ref. [21].

## References

- [1] M. Anselmino, A. Efremov and E. Leader, Phys. Rep. 261 (1995) 1; erratum *ibid* 281 (1997) 399. B. Lampe and E. Reya, hep-ph/9810270, and references therein.
- [2] R.L. Jaffe, Proceedings of the 'Ettore Majorana International School of nucleon Structure', Erice 1995. hep-ph/9602236
- [3] J. Ralston and D.E. Soper, Nucl. Phys. B 152 (1979) 109.
- [4] R.L. Jaffe, 2nd Topical Workshop 'Deep Inelastic Scattering on Polarized Targets: Physics with Polarized Targets at HERA', DESY /Zeuthen 1997. hep-ph/9710465.
- [5] N. Saito, Nucl. Phys. A 638 (1998) 575. M. Anselmino et al., Proc. of the 'Workshop on Future Physics at HERA', Hamburg 1995. hep-ph/9608393.
- [6] R.L. Jaffe and X. Ji, Phys. Rev. Lett. 67 (1991) 552; Nucl. Phys. B 375 (1992) 527.
- [7] B.-Q. Ma, I. Schmidt and J. Soer, Phys. Lett. B 441 (1998) 461.
- [8] I. Schmidt and J. Soer, Phys. Lett. B 407 (1997) 331.
- [9] S. Scopetta and V. Vento, Phys. Lett. B 424 (1998) 25; hep-ph/9707250 (1997).

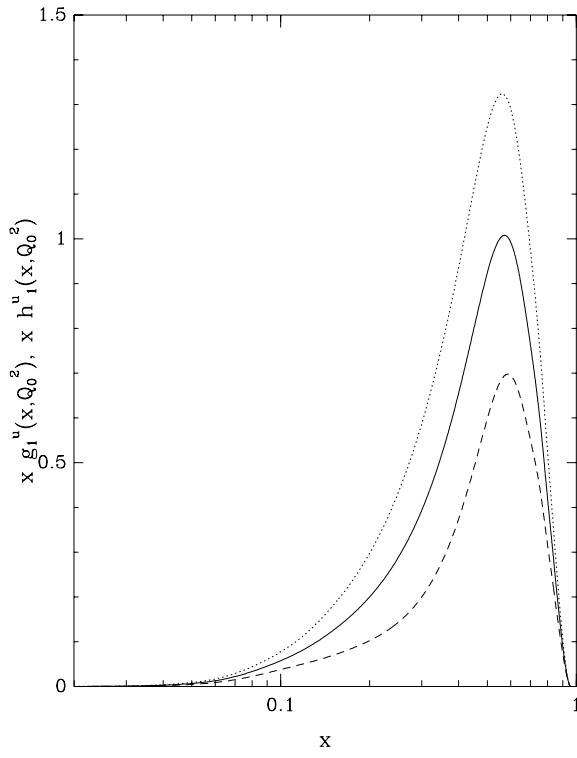
- [10] V. Barone, T. Calarco and A. D'rago, *Phys. Lett. B* 390 (1997) 287; *Phys. Rev. D* 56 (1997) 527.
- [11] C. Bourrely and J. Soer, *Nucl. Phys. B* 423 (1994) 329. P. Poblitsa and V. Polyakov, *Phys. Lett. B* 389 (1996) 350. B. J. Io e and A. Khodjamirian, *Phys. Rev. D* 51 (1995) 3373. R. Kirschner, L. Mankiewicz, A. Schafer and L. Szymanowski, *Z. Phys. C* 74 (1997) 501. R. Jakob, P. J. Mulders and J. Rodrigues, *Nucl. Phys. A* 626 (1997) 937.
- [12] X. Artru and M. Mekh, *Z. Phys. C* 45 (1990) 669.
- [13] W. Vogelsang, *Phys. Rev. D* 57 (1998) 1886. A. Hayashigaki, Y. Kanazawa and Y. Koike, *Phys. Rev. D* 56 (1997) 7350. S. Kumano and M. Miyama, *Phys. Rev. D* 56 (1997) R2504.
- [14] P. Faccioli, M. Traini and V. Vento, hep-ph/98078201. P. Faccioli, Thesis, Universita degli Studi di Trento, 1998 (unpublished).
- [15] M. Traini, V. Vento, A. Mair and A. Zambarda, *Nucl. Phys. A* 614 (1997) 472 and references therein. A. Mair and M. Traini, *Nucl. Phys. A* 624 (1997) 564.
- [16] B. D. Keister and W. N. Polyzou, *Adv. in Nucl. Phys.* 20 (1991) 225. F. Coester, *Prog. Part. Nucl. Phys.* 29 (1992) 1. J. Carbonell, B. Desplanques, V. A. Kamanov and J.-F. Mathiot, *Phys. Rep.* 300 (1998) 215.
- [17] H. M. Elsh, *Phys. Rev. D* 9 (1974) 1095. M. V. Terent'ev, *Sov. J. Nucl. Phys.* 24 (1976) 207. V. B. Berestetskii and M. V. Terent'ev, *Sov. J. Nucl. Phys.* 24 (1976) 1044; 25 (1977) 653.
- [18] M. Ferraris, M. M. Giannini, M. Pizzo, E. Santopinto and L. Tiator, *Phys. Lett. B* 364 (1995) 231.
- [19] H. L. Lai (CTEQ Coll.), *Phys. Rev., D* 55 (1997) 1280.
- [20] T. Weigand and W. Melnitchouk, *Nucl. Phys. B* 465 (1996) 267.
- [21] M. Hirai, S. Kumano and M. Miyama, *Comput. Phys. Commun.* 111 (1998) 150.
- [22] S. Caspi and N. Isgur, *Phys. Rev. D* 34 (1986) 2809. L. Ya. Glozman and D. O. Riska, *Phys. Rep.* 268 (1996) 263.
- [23] F. Cardarelli, E. Pace, G. Salmè and S. Simula, *Phys. Lett. B* 357 (1995) 267; *B* 371 (1996) 7.

## Figure captions

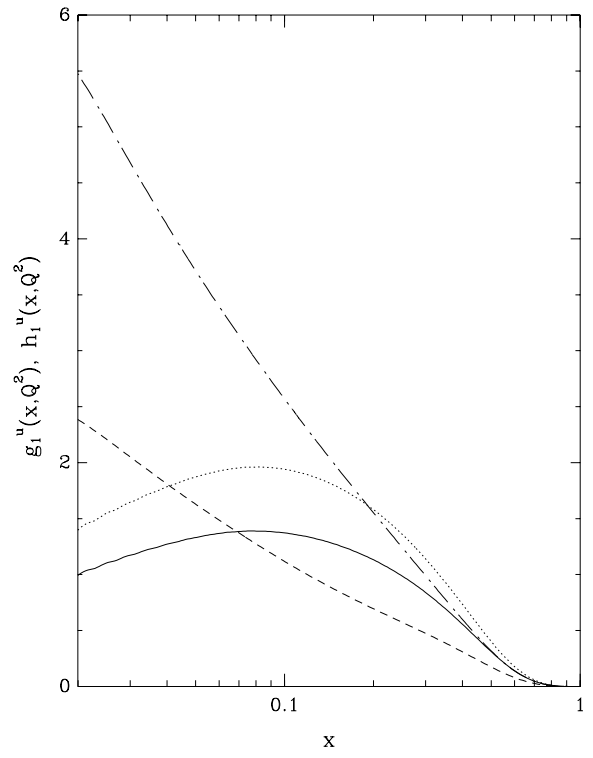
Figure 1 Helicity and transversity distributions for the u quark a) at the hadronic scale  $Q_0^2 = 0.094 \text{ GeV}^2$  and b) after evolution up to  $Q^2 = 100 \text{ GeV}^2$ . In g. a) the solid line corresponds to  $xh_1$ , the dashed line to  $xg_1$  and the dotted line is the result when Melosh rotation is not considered ( $h_1 = g_1$ ). In g. b) the solid and dashed lines represent  $h_1$  and  $g_1$  respectively. The dotted and dash-dotted lines correspond to  $h_1$  and  $g_1$  when Melosh Rotation is neglected.

Figure 2. Ratio between transverse and longitudinal asymmetries (eq (11)) as a function of the center of mass rapidity  $y$  for  $Q^2 = 100 \text{ GeV}^2$  and a center of mass energy  $\sqrt{s} = 100 \text{ GeV}$  (solid line). The dashed line corresponds to the case when the Melosh rotation is switched off. The dotted line is the result obtained in the non-relativistic model discussed in the text.

Figure 3. Ratio between transverse and longitudinal asymmetries as a function of the invariant mass of the produced lepton pair ( $Q^2$ ) for a center of mass rapidity  $y = 0$  and a center of mass energy  $\sqrt{s} = 100 \text{ GeV}$ . Notation as in g. 2.



(a)



(b)

Figure 1

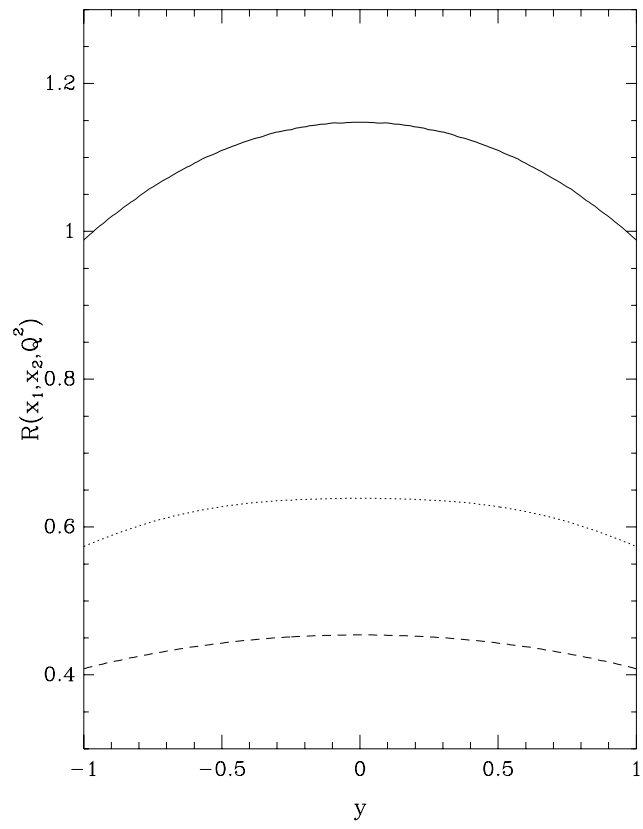


**Figure 2**

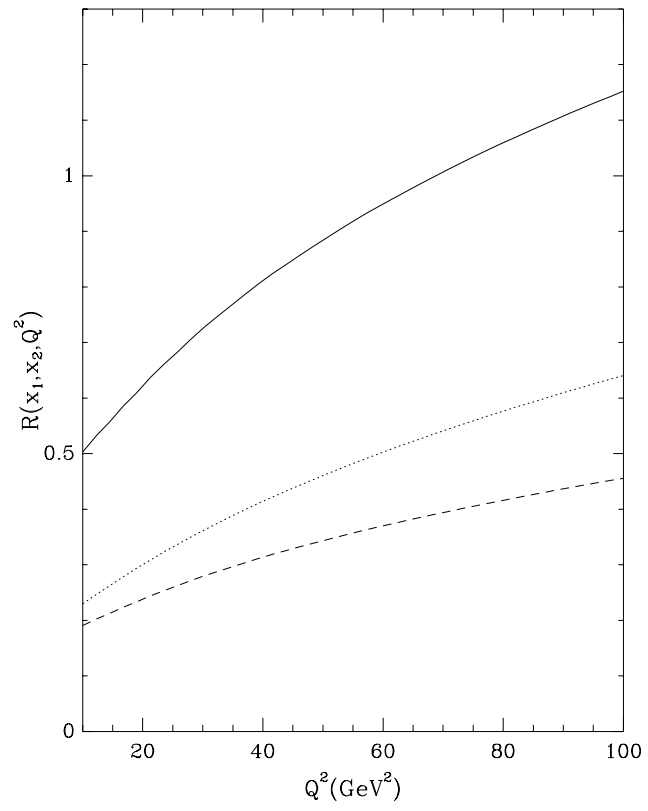


**Figure 3**